Photocatalyst of Lamellar Aggregates of RuO_x-Loaded Perovskite Nanosheets for Overall Water Splitting

Yasuo Ebina,* Nobuyuki Sakai, and Takayoshi Sasaki

Advanced Materials Laboratory, National Institute for Materials Science, 1-1 Namiki, Tsukuba, Ibaraki 305-0044, Japan

Received: April 8, 2005; In Final Form: July 21, 2005

Overall photocatalytic splitting of water was achieved using a restacked aggregate of exfoliated nanosheets of $Ca_2Nb_3O_{10}$, which was synthesized by flocculating a colloidal suspension of the nanosheets with alkali-metal ions and a trace amount of ruthenium red, a trinuclear complex of $([(NH_3)_5Ru-O-Ru(NH_3)_4-O-Ru(NH_3)_5]Cl_6$. The as-restacked material showed the evolution of H_2 gas from water immediately after UV irradiation, while O_2 evolution was observed only after some induction time, which may be understood by the possible oxidation of ruthenium red to RuO_x in the initial stage. The restacked aggregate, which was heated at 773 K to convert the ruthenium complex to the oxide, underwent the stoichiometric splitting of water upon initiation of UV illumination, verifying the hypothesis. Total decomposition of water could not be attained with the bulk layered host of $KCa_2Nb_3O_{10}$ as well as its RuO_x-loaded forms obtained via a conventional impregnation procedure. This clearly demonstrates the effectiveness of the present exfoliation−restacking route for loading RuO_x to improve and enhance the photocatalytic activities of layered semiconducting materials. A homogeneous distribution of RuO_x was suggested by XPS depth-profile analysis on the materials obtained through the exfoliation−restacking process.

Introduction

The photocatalytic splitting of water is one of the promising techniques for converting light energy into clean chemical energy. To promote the effective decomposition of water into H_2 and O_2 by a photocatalyst, its conduction band edge should be higher than the potential energy for the H^+/H_2 redox couple while its valence band edge should be lower than the O_2/H_2O potential energy. Although there are a number of semiconducting materials that satisfy these prerequisites, overall water splitting under UV irradiation has been limited to a few wide-gap semiconductors such as ZrO_2,[1] $NaTaO_3$,[2] $RbLnTa_2O_7$ (Ln = La, Nd, Sm),[3] and $A_2SrTa_2O_7$ (A = H, K, Rb).[4] Besides these exceptional cases, decomposition of water has been attained after modification of photocatalysts with cocatalysts such as Pt,[5,6] NiO_x,[7−9] and RuO_x.[10,11] It is believed that the cocatalysts act as active sites which can expedite the effective charge separation of photogenerated carriers and, thus, suppress their loss via recombination. However, more than one-half of the photocatalysts that have a potential for reduction/oxidation of water do not necessarily undergo overall water splitting, even after modification with cocatalysts. This fact highlights the importance of how cocatalysts are combined and distributed in the photocatalysts. Conventional procedures involving impregnation can load the cocatalysts only at the surface of photocatalysts. Therefore, development of a new technique is required to attain dispersion of the cocatalysts in the nanometer regime throughout the entirety of photocatalytic materials.

Recently, we reported that the photocatalytic activity of Dion−Jacobson-type layered perovskite, $KCa_2Nb_3O_{10}$, was significantly enhanced by loading Pt as the cocatalyst through the delamination−restacking process.[12] The layered oxide was exfoliated into unilamellar sheets, which were subsequently loaded with Pt nanoparticles via photodeposition. The Pt-loaded nanosheets were flocculated with alkali-metal ions to restore a layered aggregate. Through this route Pt nanoparticles can be incorporated in a highly dispersed fashion into the host lattice of the layered perovskite. The resulting material exhibited an enhanced rate of H_2 gas evolution from a methanol aqueous solution and O_2 gas evolution from a silver nitrate solution. However, overall water splitting was not accomplished without these sacrificial agents, a failure possibly associated with the chemical nature of Pt on which a back reaction proceeds very rapidly.

In the present study, the nanosheets were flocculated with a trace amount of di-μ-oxo-bridged trinuclear ruthenium complex ($[(NH_3)_5Ru-O-Ru(NH_3)_4-O-Ru(NH_3)_5]Cl_6$, ruthenium red) as well as predominant alkali-metal ions, and the photocatalytic activity of the resulting restacked compounds was studied. Stoichiometric decomposition of pure water into H_2 and O_2 gas was achieved with this system.

Experimental Section

Reagents and Materials. Niobium oxide, potassium carbonate, and calcium carbonate were of 99.99% purity (Rare Metallic Co. Ltd.). All other chemicals were of reagent grade. Milli-Q filtered ultrapure water (>18 MΩ cm) was used throughout.

$KCa_2Nb_3O_{10}$ was prepared by calcining a mixture of K_2CO_3, $CaCO_3$, and Nb_2O_5 (K:Ca:Nb = 1.1:2:3) at 1473 K for 12 h.[13] Five grams of the powder was stirred with 200 cm^3 of a HNO_3 aqueous solution (5 mol dm^{-3}) for 72 h to replace K^+ with H^+.[14] After filtration, the solid was washed with distilled water and dried in air. A resulting protonic oxide of $HCa_2Nb_3O_{10}\cdot 1.5H_2O$ (0.4 g) was dispersed in 100 cm^3 of a tetrabutylammonium hydroxide (TBAOH) aqueous solution at a molar ratio of $TBAOH/HCa_2Nb_3O_{10}\cdot 1.5H_2O = 1$. This mixture was shaken

* To whom correspondence should be addressed. Email: ebina.yasuo@nims.go.jp.

10.1021/jp051823j CCC: $30.25
Published on Web 08/23/2005

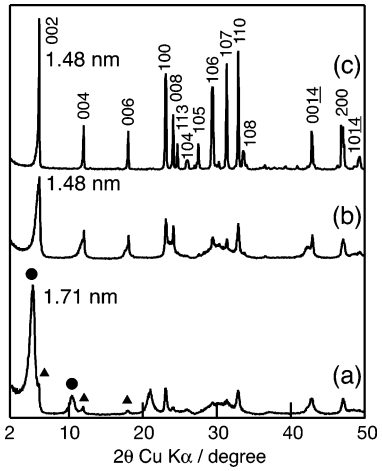

Figure 1. XRD pattern of (a) a product flocculated with K^+ ions and ruthenium red, *ex*-$Ca_2Nb_3O_{10}/K^+$/Ru, (b) sample a heat-treated at 773 K, and (c) starting bulk material, $KCa_2Nb_3O_{10}$.

at room temperature for 7 days. Our previous study confirmed the complete delamination into unilamellar nanosheets by this procedure.[12,15] The resulting colloidal suspension was added dropwise at a rate of 1 cm^3 min^{-1} into a KOH aqueous solution (2 mol dm^{-3}) containing a small amount of ruthenium red (corresponding to 0.3 wt % Ru with respect to $HCa_2Nb_3O_{10}\cdot 1.5H_2O$). The obtained precipitate was filtered, washed with water, and dried in air.

Photocatalytic Tests. Photocatalytic experiments of water splitting were carried out in an air-free closed gas circulation system with a reaction cell made of quartz (350 cm^3 capacity). A flocculated compound (0.3 g) suspended in 330 cm^3 of deionized water was introduced to the reaction cell and photoirradiated using a 450 W Hg lamp under Ar atmosphere (approximately 13 kPa). The evolved gaseous species were determined by gas chromatography (Shimadzu GC-14, MS-5A column, Ar carrier) through a gas sampler (7 cm^3) directly connected to the reaction system in order to avoid any contamination from the air.

Characterizations. X-ray diffraction (XRD) patterns were collected on a Rigaku Rint 2000S powder diffractometer with graphite monochromatized Cu Kα radiation ($\lambda = 0.154\,05$ nm). X-ray photoelectron spectra (XPS) were obtained using a Physical Electronics XPS-5700 spectrometer with the Al Kα line (1286.6 eV). UV−visible diffuse reflection spectra were recorded by a Hitachi U-4000 spectrophotometer equipped with an integration sphere detection system. Chemical analysis was carried out by completely dissolving a weighed amount of sample in a mixed acid solution of concentrated H_2SO_4 and HF, followed by determination of metal ions (alkali, Ca, Nb, and Ru) by ICP atomic emission spectroscopy.

Results and Discussion

Flocculation of Niobate Nanosheets. Mixing of the aqueous solution containing alkali-metal ions and a trace amount of ruthenium red with the colloidal suspension of $Ca_2Nb_3O_{10}$ nanosheets immediately yielded a flocculation with a deep pink color. The material obtained by flocculation with alkali-metal ions, A^+, and ruthenium red is hereafter expressed as *ex*-$Ca_2Nb_3O_{10}/A^+$/Ru. XRD data for air-dried *ex*-$Ca_2Nb_3O_{10}/K^+$/Ru indicated the reconstruction of a layered structure. There were two basal diffraction series showing an interlayer spacing of 1.71 and 1.48 nm, indicated by circles and triangles, respectively, in Figure 1a. The former predominant phase disappeared, and only the latter was present after heating the sample at 773 K for 1 h (Figure 1b). The original $KCa_2Nb_3O_{10}$ compound before delamination had a basal spacing of 1.48 nm (Figure 1c). Taking these facts into account, the two phases may be identified as a hydrated and dehydrated material.[14] No difference was found in XRD patterns of the samples flocculated with and without ruthenium red, indicating that a trace quantity of ruthenium complex or some oxide transformed from the complex upon heating did not modify the restacked structure. This does not necessarily indicate that Ru-based species were not accommodated in the restacked structure. Rather, their incorporation may be explained in terms of their low content and high flexibility of the host oxide sheets. Because the large Ru species are sparsely distributed in the gallery, the sheets can locally bend to wrap them, leaving a major area stacked at a normal distance for the accommodation of alkali-metal ions. Additional characterization by XPS provides supporting evidence for this structure, as will be described below. Similar structural aspects have been reported in various systems.[12,16] Similar restacked structures were also obtained in the synthesis using Na and Li ions as a flocculating agent (Table 1), although some differences in hydration behaviors were recognized as will be detailed later.

TABLE 1: Stoichiometry, Interlayer Spacing, and Photocatalytic Activities of RuO_x-Loaded Restacked Nanosheets (A^+: Li^+, Na^+, and K^+)

	molar ratio of $A^+/Ca_2Nb_3O_{10}$	interlayer spacing/nm: before heating	interlayer spacing/nm: after heating	evolution rate/μmol h^{-1}: H_2	evolution rate/μmol h^{-1}: O_2
ex-$Ca_2Nb_3O_{10}/Li^+$	0.73	1.76	1.42	23	7.7
ex-$Ca_2Nb_3O_{10}/Na^+$	0.99	1.69	1.68	118	56
ex-$Ca_2Nb_3O_{10}/K^+$	0.95	1.71	1.48	96	47

Elemental analysis confirmed the nearly stoichiometric incorporation of alkali-metal ions except for Li ions (Table 1). Furthermore, Ru content was found to be 0.25 wt %, which was close to the initial dose (0.3 wt %). It can be concluded from these compositional and structural data that the layered perovskite structure was reconstructed after disintegration of the bulk crystalline phase into its elementary fragments. The ruthenium complexes are accommodated and sparsely distributed in the gallery of the oxide sheets.

The restacked products exhibited a very disordered microtexture with randomly aggregated thin crystallites (see Supporting Information), reflecting their synthetic route involving exfoliation into unilamellar oxide sheets and subsequent restacking. The specific surface area was 25−30 m^2 g^{-1} for Na and K forms. The Li form had a relatively small value of 9 m^2 g^{-1}. In any case, the surface area was greatly enhanced in comparison with that (1−2 m^2 g^{-1}) of the starting bulk material, $KCa_2Nb_3O_{10}$, before delamination. This should be favorable for their use as photocatalysts.

Characterization of the Restacked Materials. Figure 2 depicts UV−visible diffuse reflection spectra for the flocculated sample, *ex*-$Ca_2Nb_3O_{10}/K^+$/Ru, which obviously support incorporation of the ruthenium complex. A strong absorption at a wavelength of 350 nm or below is characteristic of semiconducting $Ca_2Nb_3O_{10}$ nanosheets, the genuine spectrum of which is indicated by a dotted trace c. In addition to this feature the sample showed absorption peaks extending in a visible light region. The ruthenium red can account for the absorption centered at 546 nm, while the other broad peaks at 337 and 478 nm may be attributable to ruthenium brown, which is an oxidized form of ruthenium red.[17,18] Washing the as-restacked product with pure water in the filtration procedure may cause

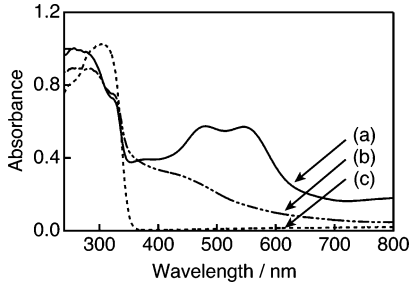

Figure 2. UV−visible diffuse reflection spectra of (a) *ex*-$Ca_2Nb_3O_{10}/K^+$ with Ru red, (b) *ex*-$Ca_2Nb_3O_{10}/K^+$ after UV irradiation in pure water for 5 h, and (c) bulk $KCa_2Nb_3O_{10}$.

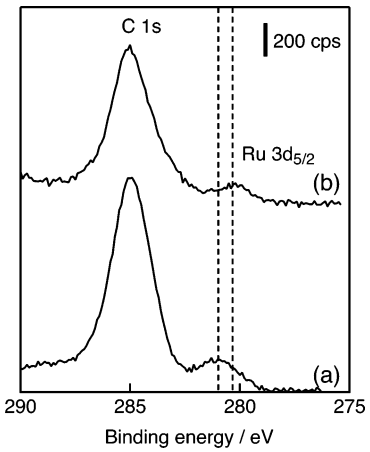

Figure 3. Narrow scan of XP spectra of (a) *ex*-$Ca_2Nb_3O_{10}/K^+$ with Ru red and (b) after heating sample a at 773 K for 1 h .

partial oxidation of the complex of ruthenium red, because the sample was exposed to a substantially lower pH in comparison with the restacking process (pH ≈ 12). It is well known that the oxidation state of the complex is very sensitive to the pH value.[19]

In XPS analysis for the as-flocculated sample containing a trace amount (0.3 wt %) of the ruthenium complex, it was difficult to discern the Ru signal due to a huge C 1s peak located in the vicinity. The signal was barely detected when the dose was increased to 1.5 wt % (Figure 3). This faint peak may be assigned as Ru $3d_{5/2}$. There should be characteristic doublet peaks due to Ru in this energy region. The other peak, Ru $3d_{3/2}$, may be buried in the strong C 1s peak. Actually, the doublet peaks were detected after sputtering by Ar^+ ions, which will be described later. The peak position of Ru $3d_{5/2}$ was 280.9 and 280.4 eV for the as-flocculated material and its heated sample, respectively, although these are approximate due to the very broad profile. The former value may be reasonable by taking into account the fact that ruthenium ammine complexes, e.g., $[Ru(NH_3)_6]Cl_3$, show a relatively high binding energy.[20] The latter is in good agreement with a chemical shift reported for ruthenium oxide.[21]

A hydration tendency of the restacked materials was examined by monitoring a change in XRD patterns upon immersion in aqueous phase. The sample heated at 773 K for 1 h was in contact with pure water for a couple of minutes, and the solid recovered by filtration was immediately followed by XRD measurement while it was in the wet state. Figure 4 illustrates changes in XRD pattern upon H_2O treatment. Despite the short duration of H_2O treatment, an increase of the interlayer distance was observed and, interestingly, the change was dependent on alkali-metal ions in the gallery. The *ex*-$Ca_2Nb_3O_{10}/Na^+$/Ru exhibited the highest hydration tendency. The sample heated at

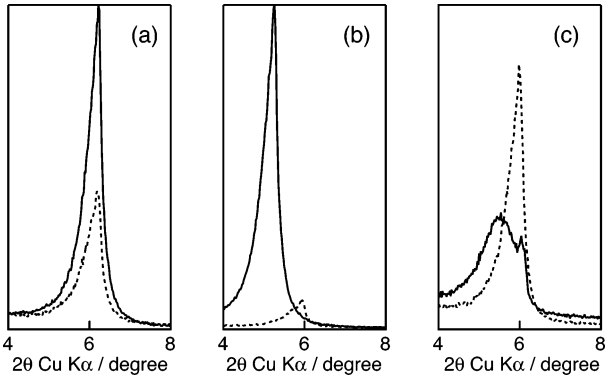

Figure 4. XRD patterns of restacked materials heated at 773 K for 1 h (dashed line) and soaked in pure water (solid line): (a) *ex*-$Ca_2Nb_3O_{10}/Li^+$/Ru, (b) *ex*-$Ca_2Nb_3O_{10}/Na^+$/Ru, and (c) *ex*-$Ca_2Nb_3O_{10}/K^+$/Ru.

773 K and cooled in air showed an XRD pattern virtually the same as the as-restacked sample (see Table 1). Their interlayer distance of ∼1.7 nm is larger than that for the dehydrated K form. The difference of ∼0.28 nm is comparable to the size of water molecules. This suggests a very fast rehydration tendency for this sample. Thus, the pattern was measured using a specially designed sample holder with an aluminum foil cover to prevent moisture uptake.[22] The data obtained in this case, in practice, showed a contracted interlayer spacing of 1.48 nm, supporting the above explanation. However, despite the care taken, the start of hydration was still recognized from the anisotropic peak profile with an apparently high intensity distribution to a lower angular range. This again indicates the extremely high hygroscopic nature of the Na form. On the other hand, the K form showed a little slower hydration, producing a predominant hydrated phase as well as the original dehydrated one in a minor amount. In contrast, the Li form did not show a marked change in XRD profile, indicating negligible hydration. These data indicated that the interlayer gallery most likely becomes hydrated at least in the Na and K forms when their photocatalytic water decomposition is examined.

Photocatalytic Reactivities. In the photocatalytic reaction tests for water splitting, a powder sample of the original layered phase $KCa_2Nb_3O_{10}$ exhibited only limited activity (3.8 μmol h^{-1}) in H_2 gas evolution and no activity in O_2. Loading of RuO_x via impregnation with ruthenium red and subsequent heating at 773 K improved the evolution rate of H_2 gas to 25.7 μmol h^{-1} in the initial 1−2 h but did not lead to O_2 generation (see Figure 5). It is noteworthy that H_2 evolution slowed with time. Blocking of the oxidation process should be responsible for this behavior. Namely, overall decomposition of water could not be attained with the Dion−Jacobson-type layered perovskite and its modified form loaded with RuO_x via the conventional procedure.

The restacked aggregate, which was obtained by flocculation with K^+ ions in the absence of ruthenium red, showed similar photocatalytic behavior, yielding only H_2 gas at a rate of 7.1 μmol h^{-1}. No evolution of O_2 gas was observed. Interestingly, incorporation of ruthenium red in the above-mentioned exfoliation−restacking process led to different results, as depicted in Figure 5. In the initial stage, only H_2 gas evolved. However, O_2 gas started to evolve after 3 h of UV irradiation, although the resulting gas yields of 27 and 9.7 μmol h^{-1} for H_2 and O_2 were not still stoichiometric. Evolution of O_2 gas after the induction time may be understood in terms of the formation of ruthenium oxide, RuO_x, as an active site. During the induction time, photogenerated positive holes may be consumed to oxidize the ruthenium complex while electrons are involved in H_2 gas

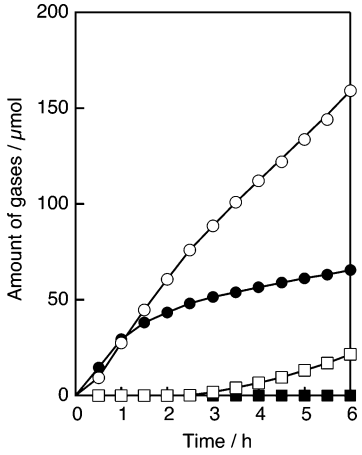

Figure 5. Time courses of gas evolution from water on (a) bulk $KCa_2Nb_3O_{10}$ loaded with RuO_x ((●) H_2 and (■) O_2) and (b) ruthenium-red-loaded material, *ex*-$Ca_2Nb_3O_{10}/K^+$/Ru ((○) H_2 and (□) O_2). Loading of RuO_x onto the bulk $KCa_2Nb_3O_{10}$ was attained by impregnation of Ru red and subsequent heating at 773 K.

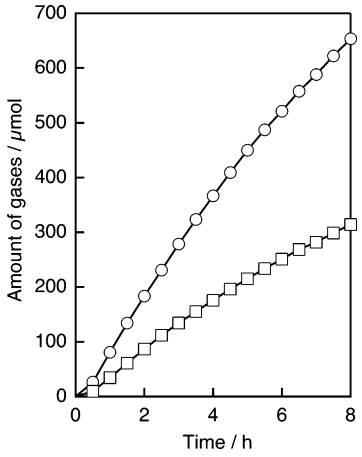

Figure 6. Time course of gas evolution from water on ruthenium-red-loaded material, *ex*-$Ca_2Nb_3O_{10}/K^+$/Ru, heat treated at 773 K: (○) H_2 and (□) O_2.

evolution. After all the ruthenium complexes are converted into ruthenium oxide, O_2 gas starts to evolve on it. In fact, the deep pink color due to the ruthenium complex faded to light gray, being compatible with this change. UV−visible data in the visible-light region changed to a broad and featureless profile, losing absorption peaks attributable to the ruthenium complex (see Figure 2b). This strongly supports the decomposition. On the other hand, XPS analysis confirmed the persistence of Ru-based species. The signal intensity, although only detectable at a loading of 1.5 wt %, was virtually similar to that before UV irradiation.

On this hypothesis, we employed the heated sample of *ex*-$Ca_2Nb_3O_{10}/K^+$/Ru as a photocatalyst. UV−visible spectra and XPS data were mostly comparable to those for the sample obtained via exposure to UV light. As described above, formation of the oxide was suggested from the chemical shift of the XPS peak of Ru $3d_{5/2}$. In this case, evolution of both H_2 and O_2 gas was observed in a stoichiometric ratio (96 and 47 μmol h^{-1}, respectively) immediately after UV irradiation (see Figure 6), indicating the total photocatalytic decomposition of water.

A marked difference in photocatalytic behavior between this sample and the bulk $KCa_2Nb_3O_{10}$ loaded with RuO_x via the conventional impregnation procedure may be attributed to the mode or degree of dispersion. The active sites of RuO_x in the

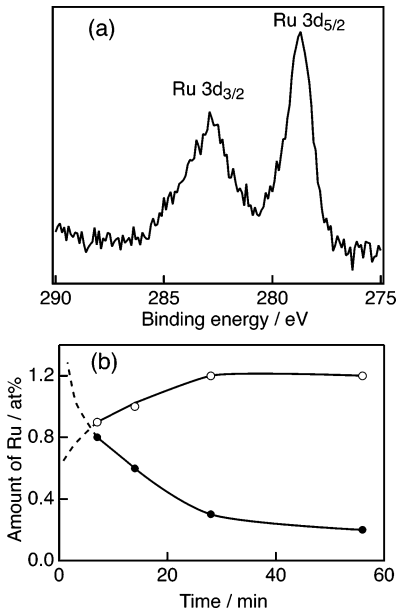

Figure 7. (a) Narrow scan of the XP spectrum after Ar^+ sputtering for 7 min on *ex*-$Ca_2Nb_3O_{10}/K^+$/Ru heated at 773 K for 1 h. (b) Ru content as a function of sputtering time: *ex*-$Ca_2Nb_3O_{10}/K^+$/Ru (○) and bulk $KCa_2Nb_3O_{10}$ by impregnation with $RuCl_3$ (●).

latter photocatalyst are expected to be present only at its surface. In contrast, RuO_x should be in the form of nanoparticles and highly dispersed throughout the photocatalyst in the restacked aggregate. In such a system, effective and rapid charge separation is expected to occur, which leads to the overall water splitting. To obtain information on the location of RuO_x, an XPS depth profile was obtained by sputtering the samples with Ar^+ ions. Sputtering for 7 min eliminated the strong peak due to C 1s and doublet peaks characteristic of Ru $3d_{3/2}$ and Ru $3d_{5/2}$ appeared (Figure 7a). Their intensity ratio of 2/3 agrees well with the literature data,[23] although their peak positions were unreliable. A significant drift was observed upon sputtering, which may be due to heavy charge-up through Ar^+ ion bombardment. Figure 7b shows a variation of the Ru content as a function of sputtering time. There is a clear difference between the material fabricated through this exfoliation−restacking process and that obtained by the conventional impregnation procedure. The former sample showed a rather constant depth profile, confirming that RuO_x is homogeneously distributed throughout the sample. A constant content of 1.2 at. % observed after sputtering for 28 min was comparable to a theoretical value of 0.9 at. % calculated from the initial dose (1.5 wt %). In contrast, RuO_x tended to be condensed near the surface in the latter material, showing decay to a negligible level with increasing sputtering time.

The Na form exhibited a higher rate of activity (Table 1), possibly due to its higher hydration ability. On the other hand, the photocatalytic activity was considerably lower for the Li^+ form and, in addition, the evolved H_2 and O_2 gases were not in a stoichiometric ratio. The lower hydration tendency may partly account for this poor activity. A possible structural degradation upon heat treatment at 773 K also may be responsible for this behavior. The Li^+ content deviated from the stoichiometry (Table 1), suggesting incomplete exchange for H^+. Liberation of the remaining H^+ as H_2O may partly destroy the layered structure.

The present study demonstrated that the exfoliation−restacking process is effective in achieving overall decomposition of pure water under UV illumination with the layered perovskite.

We expect that this approach will be applicable to a variety of layered semiconducting oxides to fabricate photocatalytic materials for overall splitting of water.

Acknowledgment. The authors thank Mr. Satoshi Takenouchi of the National Institute for Materials Science for his assistance in wet chemical analysis. This work was supported by a grant for Core Research for Evolution Science and Technology (CREST), Japan Science and Technology Agency (JST).

Supporting Information Available: SEM image of restacked products (Figure 1S). This material is available free of charge via the Internet at http://pubs.acs.org.

References and Notes

(1) Sayama, K.; Arakawa, H. *J. Phys. Chem.* **1993**, *97*, 531.
(2) Kato, H.; Asakura, K.; Kudo, A. *J. Am. Chem. Soc.* **2003**, *125*, 3082.
(3) Machida, M.; Yabunaka, J.; Kijima, T. *Chem. Mater.* **2000**, *12*, 812.
(4) Shimizu, K.; Tsuji, Y.; Hatamachi, T.; Toda, K.; Kodama, T.; Sato, M.; Kitayama, Y. *Phys. Chem. Chem. Phys.* **2004**, *6*, 1064.
(5) Tabata, S.; Nishida, N.; Masaki, Y.; Tabata, K. *Catal. Lett.* **1995**, *34*, 245.
(6) Sayama, K.; Yase, K.; Arakawa, H.; Asakura, K.; Tanaka, A.; Domen, K.; Onishi, T. *J. Photochem. Photobiol. A* **1998**, *114*, 125.
(7) Domen, K.; Kudo, A.; Onishi, T. *J. Catal.* **1986**, *102*, 92.
(8) Kudo, A.; Tanaka, A.; Domen, K.; Maruya, K.; Aika, K.; Onishi, T. *J. Catal.* **1988**, *111*, 67.
(9) Takata, T.; Furumi, Y.; Shinohara, K.; Tanaka, A.; Hara, M.; Kondo, J. N.; Domen, K. *Chem. Mater.* **1997**, *9*, 1063.
(10) Inoue, Y.; Kubokawa, T.; Sato, K. *J. Phys. Chem.* **1991**, *95*, 4059.
(11) Kohno, M.; Kaneko, T.; Ogura, S.; Sato, K.; Inoue, Y. *J. Chem. Soc., Faraday Trans.* **1998**, *94*, 89.
(12) Ebina, Y.; Sasaki, T.; Harada, M.; Watanabe, M. *Chem. Mater.* **2002**, *14*, 4390.
(13) (a) Dion, M.; Ganne, M.; Tournoux, M. *Mater. Res. Bull.* **1981**, *16*, 1429. (b) Jacobson, A. J.; Johnson, J. W.; Lewandowski, J. T. *Inorg. Chem.* **1985**, *24*, 3727.
(14) Jacobson, A. J.; Lewandowski, J. T.; Johnson, J. W. *J. Less-Common Met.* **1986**, *116*, 137.
(15) Ebina, Y.; Sasaki, T.; Watanabe, M. *Solid State Ionics* **2002**, *151*, 177.
(16) Wang, L. Z.; Sakai, N.; Ebina, Y.; Takada, K.; Sasaki, T. *Chem. Mater.* **2005**, *17*, 1352.
(17) Fletcher, J. M.; Greenfield, B. F.; Hardy, C. J.; Scargill, D.; Woodhead, J. L. *J. Chem. Soc.* **1961**, 2000.
(18) Ruthenium brown can be formulated as $Ru^{IV}-O-Ru^{III}-O-Ru^{IV}$, which is formed by oxidation via elimination of one electron from the ruthenium red: $Ru^{III}-O-Ru^{IV}-O-Ru^{III}$. See refs 17 and 19.
(19) Geselowitz, D. A.; Kutner, W.; Meyer, T. J. *Inorg. Chem.* **1986**, *25*, 2015.
(20) Shepherd, R. E.; Proctor, A.; Henderson, W. W.; Myser, T. K. *Inorg. Chem.* **1987**, *26*, 2440.
(21) Ogura, S.; Sato, K.; Inoue, Y. *Phys. Chem. Chem. Phys.* **2000**, *2*, 2449.
(22) The damped intensity of the basal peak is ascribed to the measurement using the holder with an Al cover. All other data were obtained in air.
(23) Siegbahn, K.; Nording, C.; Fahlman, A.; Nordberg, R.; Hamrin, K.; Hedman, J.; Johansson, G.; Bergmark, T.; Karksson, S. E.; Lindgern, I.; Lindberg, B. *ESCA Atomic, Molecular and Solid State Structure Studied by Means of Electron Spectroscopy*; Almqvist & Wilksells: Uppsala, 1967.